



# Analysis of Spatial Variability of Soil Parameters in Thick Loess-Filled Stratum

Luxi Li\*, Gong Liu, Yuanyuan Zhang, Weizhong Lai

School of Civil Engineering, Lanzhou Jiaotong University Lanzhou China

\*Email address: 971458232@qq.com, Telephone number: 18794877895

**Abstract.** This paper investigates the data obtained from field tests and laboratory geotechnical experiments. Based on the semi-variogram method theory and the establishment of a random field model foundation, the data is detrended, followed by verifying stationarity and ergodicity. We comparatively analyze three models using the semi-variogram method to calculate fluctuation ranges and determine spatial variation coefficients. Finally, the covariance matrix decomposition method is employed to construct the random field model, thereby achieving spatial variability analysis of soil parameters in thick loess-filled strata. The main conclusions are: (1) The spherical model demonstrates the highest probability (80%) among optimal mathematical models, suggesting priority consideration for fluctuation range calculations. (2) Variation coefficient analysis reveals medium variability in compression modulus, weak variability in shear wave velocity, cohesion, natural density, and internal friction angle. (3) The covariance matrix decomposition method proves most appropriate for establishing this random field.

**Keywords:** Loess; Spatial Variability; Random Field Theory;

## 1 Introduction

With the rapid urbanization in China, the scarcity of urban land resources has become a critical issue, leading to conflicts between construction demands and available land resources. Consequently, artificial mountain excavation and soil filling for land creation have emerged as a solution. In Northwest China, characterized by extensive loess regions with highly eroded gullies and ravines, large-scale high-fill engineering projects are extensively implemented. However, the excavation process disrupts the natural structure of loess, resulting in inherent poor homogeneity. Further compounded by diverse filling methods, thick filled loess strata exhibit significant spatial variability. Additionally, the high compressibility of loess induces substantial settlement, contributing to a series of engineering accidents. Therefore, stability analysis of thick high-filled loess strata has become critically important for ensuring engineering safety.

In recent years, significant attention has been directed toward the spatial variability of geotechnical parameters, with researchers proposing the application of soil property profile random fields<sup>1,2</sup> for such analyses. Wang et al.<sup>3</sup> developed a reliability design

method based on Monte Carlo simulation, offering transparent modeling of geotechnical uncertainties and algorithms for designers, while enabling intuitive simulation of spatial variability characteristics in soil parameters through random field theory. Li et al.<sup>4</sup> established a conditional random field theory framework grounded in random field principles and integrated it into the characterization of geotechnical parameter uncertainties. Tang Huiming et al.<sup>5</sup> investigated the granulometric composition of slip zone soils through multi-borehole spatial sampling, revealing the comprehensive characteristics and spatial variability of loess landslide zones. Yang Jian et al.<sup>6</sup> calculated pile foundation bearing capacity under spatial variability constraints, demonstrating that uncertainty increases with rising coefficients of variation and correlation distances, following a normal distribution. Su Ren et al.<sup>7</sup> studied thick collapsible loess strata in Lanzhou using field data from Metro Line 3 Phase I and validated their findings through laboratory experiments. Ching et al.<sup>8</sup> explored the mean and standard deviation of shear strength in spatially variable soils under uniform stress conditions. Zhang Mingdong<sup>9</sup> Considering the variability of geological strata, map the simulated soil distribution to the FLAC3D model for shallow foundation bearing capacity research. Wang Shuguang et al.<sup>10</sup> identified that soil cohesion conforms to the Gaussian model in random fields, with bearing capacity exhibiting significant variations corresponding to cohesion changes. Xiao Zhuoying<sup>11</sup> highlighted the impact of correlations among soil parameters on engineering reliability in urban construction. Liao Yihan<sup>12</sup>, based on the Baoji-Zhongwei Railway project, concluded that results from the semi-variogram and correlation function methods align closely, whereas the recursive spatial method yields smaller values. Chen Xiqi<sup>13</sup> analyzed the collapsibility of thick loess strata considering soil parameter variability. Lei Ling et al.<sup>14</sup>, utilizing the YanQianhu Station foundation pit project in Jinan Metro as a case study, incorporated random field theory to examine deformation mechanisms and the influence of spatial variability on soil behavior. Zhao Chao<sup>15</sup> Simultaneously considering the variability of geological strata and soil parameters, a probability modeling method based on random field theory is proposed to couple the spatial distribution of soil types and parameters. Zhu Lei<sup>16</sup> demonstrated that slope reliability decreases with increasing height when cohesion variability diminishes under spatial variability considerations, whereas reliability increases with height for higher cohesion coefficients when variability is neglected.

In summary, domestic research has achieved notable progress in understanding deformation mechanisms and characteristics of high-fill engineering. However, studies addressing the complex settlement of thick strata and spatial variability of soil parameters in loess hill-gully regions subjected to mountain-cutting and gully-filling projects remain limited. This paper investigates the spatial variability of soil properties through a case study of Phase I of the Gansu Provincial Center for Disease Control and Prevention Public Health Center project. The study area features a terrain sloping from northwest to southeast, flanked by low hills, with original gullies and ridges leveled during construction, resulting in an overall broad and flattened site. Based on geotechnical exploration, the subsurface stratigraphy is delineated as follows (from top to bottom): (1) Plain Fill Layer (Q4m1): Distributed across the entire site, formed by artificial leveling, with thickness ranging from 1.0 to 23.6 m. (2) Malan Loess Layer (Q3eol): Ubiquitous in the area, buried at depths of 1.0-23.6 m and thicknesses of 63.2-92.2 m. (3)

Silty Clay (Q3al+pl): Located at depths of 80.3-93.0 m, with thicknesses of 2.0-10.5 m.  
 (4) Gravelly Sand Layer (Q1al+pl): Buried at 87.2-99.0 m, thicknesses of 2.0-20.4 m.  
 (5) Interbedded Silty Clay (Q1al+pl): Present in most boreholes, thicknesses of 1.0-9.0 m.  
 (6) Highly Weathered Mudstone: Found at depths of 95.0-111.9 m, with an exposed thickness of 3.1-6.8 m.

## 2 Random Field Theory

### 2.1 Random Field Medol

The random field model is very suitable for characterizing the spatial variability of soil because of the differences and correlations between soil parameters in different spatial positions. Its basic characteristics are mainly the mean function, the variance function, the correlation function and the covariance function. where the mean function: for the random field  $\{X(t)\}$ , if its one-dimensional distribution function is  $F(x,t)$  and the corresponding probability density function is  $f(x,t)$ , then the mean function of the random field  $\{X(t)\}$  can be defined  $\mu_x(t)$ :

$$\mu_x(t) = E[X(t)] = \int x dF(x,t) = \int x f(x,t) dx, t \in T \quad (1)$$

where T is the set of random vector t in a random field, and there is any  $t \in T$ .

the variance function: for the random field  $\{X(t)\}$ , similarly, if its one-dimensional distribution function is  $F(x,t)$  and the corresponding probability density function is  $f(x,t)$ , then the variance function  $\sigma_x^2(t)$  of the random field  $\{X(t)\}$  can be defined as:

$$\begin{aligned} \sigma_x^2(t) &= D[X(t)] = E\{X(t) - E[X(t)]\}^2 \\ &= E\{X(t)\}^2 - \{E[X(t)]\}^2 \\ &= \int \{x - E[X(t)]\}^2 dF(x,t) \\ &= \int \{x - E[X(t)]\}^2 f(x,t) dx, t \in T \end{aligned} \quad (2)$$

Standard deviation  $\sigma_x(t)$ : indicates the degree of deviation of the random field  $\{X(t)\}$  from the mean function.

Correlation function: For the random field  $\{X(t)\}$ , if its two-dimensional distribution function is  $F_{t_1 t_2}(x_1, x_2)$  and the corresponding probability density function is  $f_{t_1 t_2}(x_1, x_2)$ , then the correlation function  $R(t_1, t_2)$  of the random field  $\{X(t)\}$  is

$$\begin{aligned} R(t_1, t_2) &= E[X(t_1)X(t_2)] \\ &= \iint x_1 x_2 dF_{t_1 t_2}(x_1, x_2) \\ &= \iint x_1 x_2 f_{t_1 t_2}(x_1, x_2) dx_1 dx_2, t_1, t_2 \in T \end{aligned} \quad (3)$$

where  $T$  is the set of random vectors  $t$  in a random field, with any  $t_1, t_2 \in T$ . The correlation function  $R(t_1, t_2)$ , also known as the correlation function, is essentially the second-order mixed origin moment of  $R(t_1)$  and  $R(t_2)$ .

Covariance function: For the random field  $\{X(t)\}$ , similarly, if its two-dimensional distribution function is  $F_{t_1, t_2}(x_1, x_2)$  and the corresponding probability density function is  $f_{t_1, t_2}(x_1, x_2)$ , then the covariance function  $C(t_1, t_2)$  of the random field  $\{X(t)\}$  is:

$$\begin{aligned}
 C(t_1, t_2) &= E\left\{ [X(t_1) - E(X(t_1))] [X(t_2) - E(X(t_2))] \right\} \\
 &= \iint [x_1 - E(X(t_1))] [x_2 - E(X(t_2))] f_{t_1, t_2}(x_1, x_2) \\
 &= \iint [x_1 - E(X(t_1))] [x_2 - E(X(t_2))] f_{t_1, t_2}(x_1, x_2) dx_1 dx_2, t_1, t_2 \in T
 \end{aligned}
 \tag{4}$$

The correlation function  $C(t_1, t_2)$ , also known as the autocovariance function, is essentially a second-order mixed central moment of  $R(t_1)$  and  $R(t_2)$ .

## 2.2 Stationarity of Random Fields and Ergodicity of Various States

**2.2.1 Stationarity.** Stationarity requires that the soil parameters studied are uniform within the study range, that is, the statistical characteristics of the random field on the soil parameters will not change with the position coordinates of the soil profile. For a random field  $\{X(t), t \in T\}$  with an infinite family of distribution functions, there are any  $n, t_1, \dots, t_n \in T, t_1 + \Delta t, \dots, t_n + \Delta t \in T (\Delta t > 0)$

$$F_{t_1 + \Delta t, \dots, t_n + \Delta t}(x_1, \dots, x_n) = F_{t_1, \dots, t_n}(x_1, \dots, x_n)
 \tag{5}$$

If the joint distribution function of the random vector  $X$  is the same as that of the random vector  $X$ , then the random field  $\{X(t), t \in T\}$  is said to have strict stationarity, which is usually referred to as a strict stationary random field or strong stationary random field. If a random field has both strict stationarity and the properties of a second-order moment field, it cannot be proven to be a strict stationary random field; at this point, the concept of wide-sense stationary random fields is introduced. For a random field  $\{X(t)\}$  that has the property of a second-order moment field, if it satisfies that for any  $t \in T$ , there exists  $k$  (a constant), and for any  $t \in T; t + \Delta t \in T$ , the correlation function value  $R(t, t + \Delta t)$  depends only on  $\Delta t$  and not on  $t$ . Then this random field  $\{X(t)\}$  with the property of a second-order moment field is said to have wide-sense stationarity. It can usually be referred to as a wide-sense stationary random field or weakly stationary random field. The random fields used in this article to express the variability of soil can all be considered as wide-sense stationary random fields.

**2.2.2 Ergodicity.** The ergodicity of each state means that the statistical properties of any one sample in the random field can reflect the statistical properties of the entire random field. If there is a random field, in which the statistical properties of any one of the sample functions can reflect the statistical properties of the overall random field, then the random field is said to have the permanence of various states, and for a mean

square continuous stationary random field  $\{X(t), t \in T\}$ , the average depth  $\langle X(t) \rangle$  along the direction of depth H is:

$$\langle X(t) \rangle = \lim_{H \rightarrow \infty} \frac{1}{H} \int_0^H X(t) dt \tag{6}$$

### 3 Spatial Variability Analysis

#### 3.1 Detrending

Soil parameters generally have both trend and discrete types, the trend is the trend component, and the discrete type is the fluctuation component, that is to say, the soil parameters are composed of the trend component and the fluctuation component. According to the Vanmarcke random field theory, the fluctuation component accounts for the main influence. Therefore, only the fluctuation component of the soil parameters needs to be obtained during detrending.

$$X(z) = T(z) + F(z) \tag{7}$$

where  $z$  is the depth,  $T(z)$  is the trend component, and  $F(z)$  is the fluctuation component.

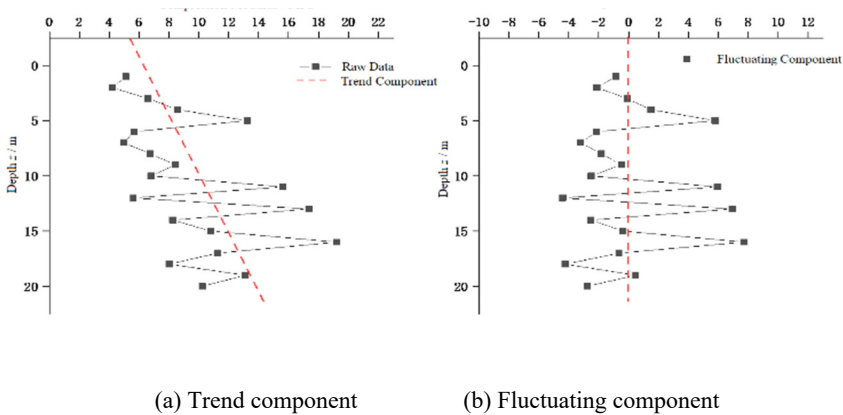


Fig. 1. Compressive modulus trend component and fluctuating component

As can be seen from Figure 1a, the compressive modulus tends to change significantly with the increase of soil depth, and Figure 1b is obtained by using MATLAB software using Formula 7 for data processing.

#### 3.2 Stationarity and Various States Have Been Tested

In the stationarity test, for any kind of soil parameter in any borehole, the set average of the random variable  $X(z_j)$  at any depth  $z_j$  is:

$$\mu_X(z_j) = \lim_{N \rightarrow \infty} \frac{1}{N} \sum_{i=1}^N X_i(z_j) = E[X(z_j)], (j = 1, 2, \dots, m) \tag{8}$$

If the depth difference between any two points is  $\Delta z$ , then the correlation function between the random variable  $X(z_j)$  and  $X(z_j + \Delta z)$  at these two points is:

$$R_X(z_j, z_j + \Delta z) = \lim_{N \rightarrow \infty} \frac{1}{N} \sum_{i=1}^N X_i(z_j) X_i(z_j + \Delta z), (j = 1, 2, \dots, m) \tag{9}$$

In equations (8) and (9),  $N$  represents the number of drilled holes;  $m$  indicates the number of samples taken in any one borehole. In practice,  $N$  and  $m$  are finite values.

Equations (8) and (9) are used to calculate the set average value and correlation function, and then the scatter plot 3.2 is plotted, through which the change of the average value and correlation function with depth can be observed, and if the change is not obvious, the parameter can be considered to meet the stationarity. Take compressive modulus as an example figure 2:

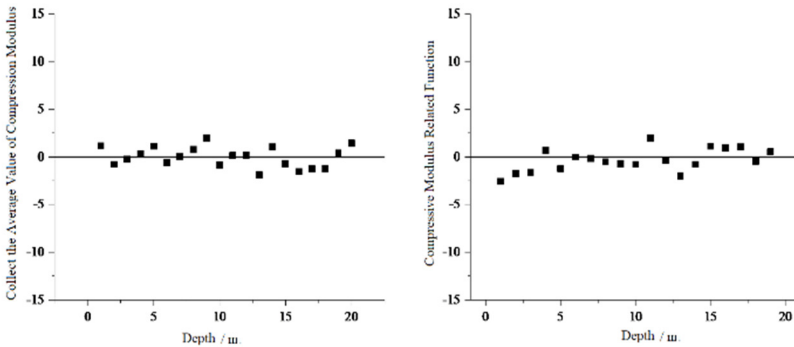


Fig. 2. Compressive modulus

In the empirical test of each state, for the original data  $X_i(z)$  of any kind of soil parameter in any borehole, the mean value along the depth is:

$$\langle X_i(z_j) \rangle = \lim_{m \rightarrow \infty} \frac{1}{m} \sum_{j=1}^m X_i(z_j) \stackrel{a.s.}{=} \mu_X(z) = E\{X(z)\}, (i = 1, 2, \dots, N) \tag{10}$$

If the difference in depth between any two points is  $\Delta z$ , the mean value of the correlation function  $X_i(z_j)X_i(z_j + \Delta z)$  along the depth is:

$$\begin{aligned} & \langle X_i(z_j)X_i(z_j + \Delta z) \rangle \\ & = \lim_{m \rightarrow \infty} \frac{1}{m} \sum_{j=1}^m [X_i(z_j)X_i(z_j + \Delta z)] \stackrel{a.s.}{=} R_X(\Delta z), (i = 1, 2, \dots, N) \end{aligned} \tag{11}$$

In equations (10) and (11): N represents the number of drilled holes; m indicates the number of samples taken in any one borehole.

Equations (10) and (11) calculate the depth mean and depth correlation functions, and Figure 3 is a scatter plot.

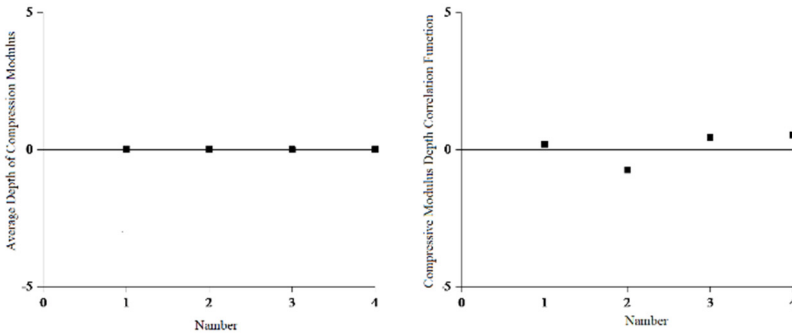


Fig. 3. Compressive modulus

### 3.3 Semivariogram Method

Following the verification of stationarity and ergodicity for soil parameters, the calculation of fluctuation scale becomes essential for characterizing spatial variability. While multiple approaches exist for this purpose (including correlation function method, recursive space method, mean zero-crossing interval method, and semi-variogram method), the semi-variogram method is uniquely advantageous due to its reduced sample size requirements and flexibility in sampling spacing. Given the typically limited availability of in-situ soil parameter data, this study exclusively employs the semi-variogram method for fluctuation scale determination.

The volatility range  $\delta$  is defined as:

$$\delta = \lim_{H \rightarrow \infty} H\Gamma^2(H) \tag{12}$$

The sample size of the soil parameter is denoted as the sample size of the soil parameter m, so that  $h=j \Delta z, j = (0, 1, \dots, m-1)$ , and the semi variogram value  $\gamma^*(h)$  is calculated according to equations (12):

$$\gamma^*(h) = \gamma^*(j\Delta z) = \frac{1}{2(m-j)} \sum_{i=1}^{m-j} [X(z_{i+j}) - X(z_i)]^2 \tag{13}$$

The  $\gamma^*(h)\sim h$  correspondence is fitted with a spherical model, an exponential model and a Gaussian model, and the function model corresponding to the curve with the greatest degree of similarity is selected. As can be seen from Eq. (2.7), when  $j$  increases, the spacing  $h$  increases correspondingly, which reduces the accuracy of the model, so we only use the first quarter of the curve. The larger the coefficient of determination, the greater the similarity of the fitting curve, and the semivariogram fitting results of each borehole are shown in Table 1. In the table, A represents the spherical model, B represents the exponential model, and C represents the Gaussian model.

**Table 1.** Semivariogram fitting results

Soil parameters	Unit	Coefficient of determination R <sup>2</sup> /%					
		Drilling 1			Drilling 2		
		A	B	C	A	B	C
Compressive modulus	MPa	71.12	87.52	82.10	89.75	96.53	75.06
Natural density	g/cm <sup>3</sup>	99.95	96.58	93.04	99.89	98.03	89.66
Cohesion	kPa	83.76	77.69	68.15	87.53	70.02	63.49
Internal friction angle	°	93.70	84.58	87.49	91.65	73.51	80.37
Shear wave velocity	m/s	96.40	87.12	10.00	97.58	90.17	81.36
Soil parameters	Unit	Coefficient of determination R <sup>2</sup> /%					
		Drilling 3			Drilling 4		
		A	B	C	A	B	C
Compressive modulus	MPa	99.23	71.58	53.84	91.17	77.05	62.57
Natural density	g/cm <sup>3</sup>	99.08	99.91	96.72	98.48	92.01	91.36
Cohesion	kPa	82.19	53.33	67.21	76.09	57.64	70.19
Internal friction angle	°	88.04	81.74	91.32	89.06	70.26	78.31
Shear wave velocity	m/s	98.54	89.23	73.06	95.88	85.72	86.30

For the compressive modulus, the spherical model, exponential model, and Gaussian model accounted for 50%, 50%, and 0% of the optimal function models, respectively. For natural density, the spherical model, exponential model, and Gaussian model accounted for 75%, 25%, and 0% of the optimal function models, respectively. For cohesion, the spherical model, exponential model, and Gaussian model accounted for 100%, 0%, and 0% of the optimal function models, respectively. For the internal friction angle, the spherical model, exponential model and Gaussian model accounted for 75%, 0% and 25% as the optimal function models, respectively. For the shear wave velocity, the spherical model, exponential model, and Gaussian model account for 100%, 0%, and 0% of the optimal function models, respectively. It can be seen that the spherical model and exponential model are suitable for compressive modulus and natural density, the spherical model and Gaussian model are suitable for soil mass mechanical parameters, the spherical model is suitable for shear wave velocity, and the spherical model is the optimal model.

Table 2 can be obtained by selecting a suitable model to calculate the fluctuation range, and the relationship between the fluctuation range of each parameter is as follows: natural density > internal friction angle > cohesion > compressive modulus, and the fluctuation range of soil parameters in the four selected boreholes is not large, so it is considered that the fluctuation range of soil parameters in this area is stable.

**Table 2.** Range of fluctuations in soil parameters

Soil parameters	Fluctuation range/m				Average value
	Drilling 1	Drilling 2	Drilling 3	Drilling 4	
Compressive modulus	2.76	1.99	2.25	2.46	2.37
Natural density	6.14	5.98	5.21	4.90	5.56
Cohesion	3.77	3.29	2.86	3.33	3.31
Internal friction angle	3.92	3.07	4.16	4.23	3.85
Shear wave velocity	2.91	3.14	3.16	2.85	3.02

### 3.4 Analysis of Spatial Variability of Filling Parameters

The spatial coefficient of variation of each parameter is calculated from Equation 14 and Table 3 is obtained.

$$C_v' = C_v \sqrt{\frac{\delta}{h}} \quad (14)$$

where  $\delta$  denotes the fluctuation range;  $h$  indicates the depth of sampling.

**Table 3.** Spatial coefficient of variation

Soil parameters	Spatial coefficient of variation				
	Drilling 1	Drilling 2	Drilling 3	Drilling 4	Average value
Compressive modulus	0.1332	0.1009	0.1016	0.1158	0.1129
Natural density	0.0358	0.0411	0.0376	0.0348	0.0373
Cohesion	0.0926	0.0874	0.0910	0.0978	0.0922
Internal friction angle	0.0546	0.0679	0.0695	0.0829	0.0687
Shear wave velocity	0.0713	0.0705	0.0727	0.0732	0.0719

It can be seen from the table that the coefficient of spatial variation of the compressive modulus is the largest, with a maximum value of 0.1332 and an average value of 0.1129, followed by the mechanical properties of the parameters cohesion and internal friction angle, the average values of which are 0.0922 and 0.0687, respectively. The maximum spatial coefficient of variation is 0.0411 and the average value is 0.0373, which is 67% lower than the average compressive modulus of 0.1129. According to the literature<sup>17</sup>, the degree of variation is classified as shown in Table 4, where the compression modulus is moderately variable, and the shear wave velocity, natural density, cohesion, and internal friction angle are all weakly variable.

**Table 4.** Degree of variation in soil parameters<sup>[17]</sup>

Coefficient	<0.1	0.1~1	≥1
Degree of variation	Weak variation	Moderate variability	Strong mutation

### 4 Establish a Random Field

The stochastic field theory covariance matrix factorization method (Equation 15) was used to simulate the spatial variability of soil parameter  $X(t)$ . The correlation function of this method can represent the correlation between any two points within the layer.

$$\ln X(t) = \mu_{\ln X(t)} \cdot I + \sigma_{\ln X(t)} \cdot L \cdot \Phi \tag{15}$$

where  $\mu_{\ln X(t)}$  and  $\sigma_{\ln X(t)}$  are the mean and standard deviations of  $\ln X(t)$ , which can be calculated according to equations (16) and (17), respectively;  $I=[1, \dots, 1]^T$  is a one-dimensional vector in which all the elements in a column of  $n$  rows are 1;  $\Phi=[\phi_1, \phi_2, \dots, \phi_n]$  is a one-dimensional standard Gaussian column vector in a column of  $n$  rows;  $L$  is a trigonometric matrix under  $n$  rows and  $n$  columns obtained by the correlation function matrix  $R$  of equation (18) by Cholesky decomposition.

$$\mu_{\ln X(t)} = \ln \mu_{X(t)} - \sigma_{\ln X(t)}^2 / 2 \tag{16}$$

$$\sigma_{\ln X(t)} = \sqrt{\ln \left[ 1 + \left( \sigma_{X(t)} / \mu_{X(t)} \right)^2 \right]} \tag{17}$$

$$R_{ij} = R_{X_i X_j}(\tau_x, \tau_y, \tau_z) \tag{18}$$

Taking the compressive modulus as an example, taking the transverse correlation distance  $\delta x$  and the longitudinal correlation distance  $\delta y$  as 20 times of the vertical correlation distance  $\delta z$ , a four-dimensional random field model with  $x, y,$  and  $z$  three-dimensional coordinates superimposed on one-dimensional color mapping discrete parameter values (Figure. 4) is established. In the past, the four-dimensional diagram of the stratified average compressive modulus of random variables without considering the spatial variability of soil parameters is shown in Figure 5, which can be obtained:

(1) Within the correlation distance, the soil parameters affect each other due to their autocorrelation, and this influence weakens with the increase of distance, and after the correlation distance is exceeded, it is considered that the soil parameters no longer affect each other.

(2) The influence of the autocorrelation of soil parameters in the plane direction is less than that in the vertical direction, but the spatial variability of soil parameters cannot be ignored.

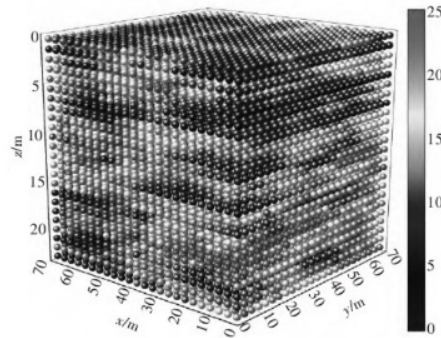


Fig. 4. Random Field Model of  $\delta x = \delta y = 20\delta z$

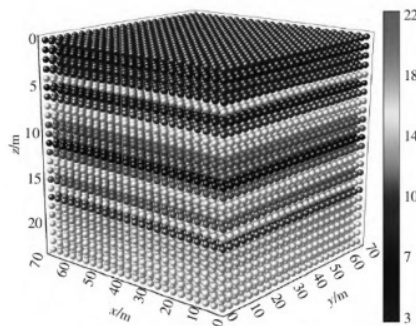
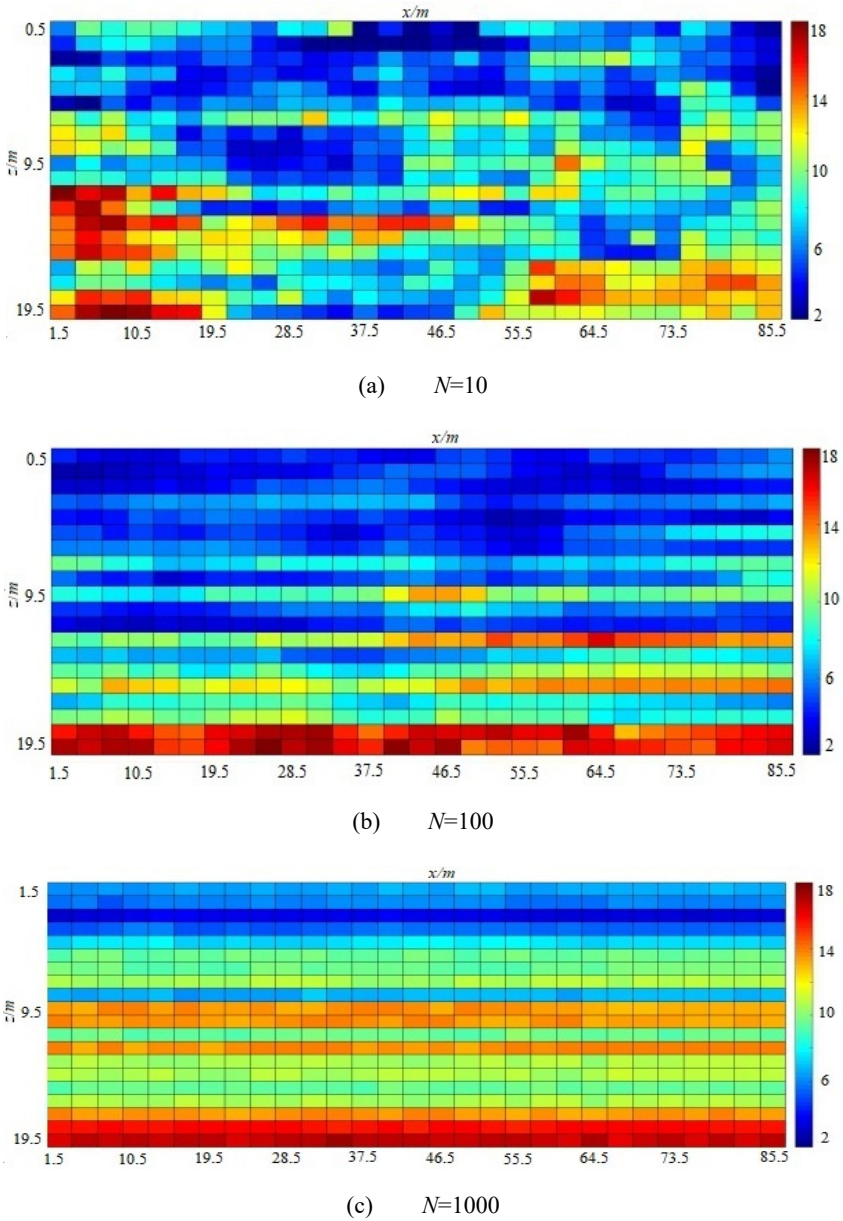


Fig. 5. Hierarchical averaging model

## 5 Simulation of Spatial Variability of Soil Parameters and Electron Microscopy Scanning

By using covariance matrix decomposition method and programming with MATLAB, the discrete values of soil parameters in random fields can be calculated, and the fluctuation range is the key factor determining the discreteness of random fields. In practical engineering, the fluctuation range in the horizontal direction is larger than that in the vertical direction. Therefore, assuming a relationship of  $\delta_x = N\delta_y$ , between the horizontal fluctuation range and the vertical fluctuation range, taking  $N=10, 100$ , and  $1000$ , the random discrete values of soil parameters under different  $N$  values are calculated using MATLAB program.

Random field simulation is performed on the soil parameters of the fill layer, and the discrete values of each soil parameter are calculated using covariance matrix decomposition method. Taking the compression modulus as an example, the distribution of the random field is simulated using MATLAB program,  $N=10$ . The simulation results of  $100, 500$ , and  $1000$  are shown in Figure 6.



**Fig. 6.** Results of covariance matrix simulation under different  $N$  values

For the random field simulation of soil parameters in the fill layer and loess layer, the discrete values of each soil parameter were calculated using covariance matrix decomposition method. Taking the compression modulus as an example, the distribution of the random field was simulated using MATLAB program. The simulation results for  $N=1000$  are shown in Figure 7.

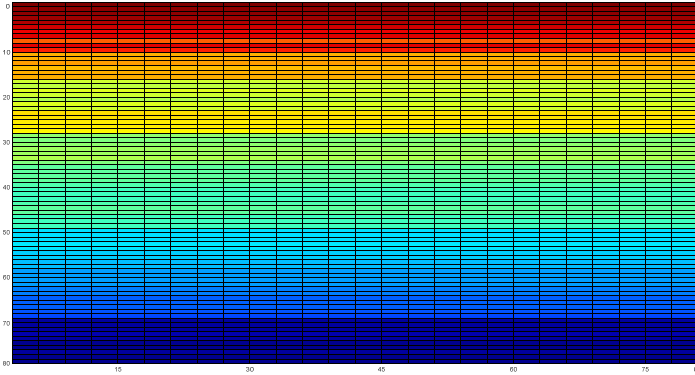
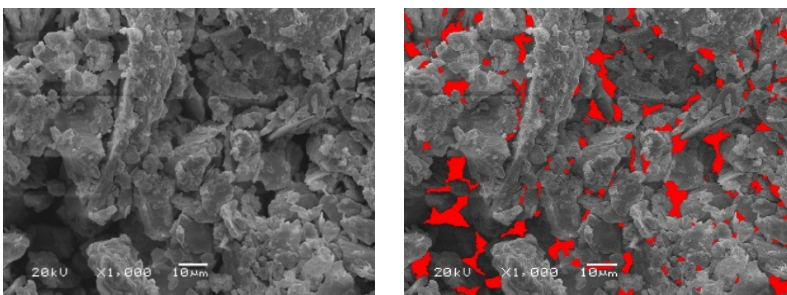


**Fig. 7.** Results of covariance matrix simulation under  $N=1000$  values

Taking the compression modulus of soil parameters as an example, the discrete values simulated by random field have randomness. Based on the simulation results of  $N=10$ , 100, and 1000, it can be concluded that the discrete values of the compression modulus with respect to the field do not show a significant trend of change in the depth direction. However, in the horizontal direction, as the value of  $N$  increases, the simulated values gradually tend to be consistent. When  $N=1$ , the simulated values of soil parameters in the horizontal direction appear chaotic and disordered, with significant differences between them; When  $N=1000$ , the simulated values in the horizontal direction tend to be consistent, and the simulated values are almost the same. Analyzing the reasons, in the case of a small  $N$  value, the fluctuation range of soil parameters in the horizontal direction is small, resulting in a lack of regularity in the simulation results of random fields. But when the value of  $N$  increases to a certain extent, the horizontal fluctuation range also increases, making the simulation results begin to show a certain regularity.

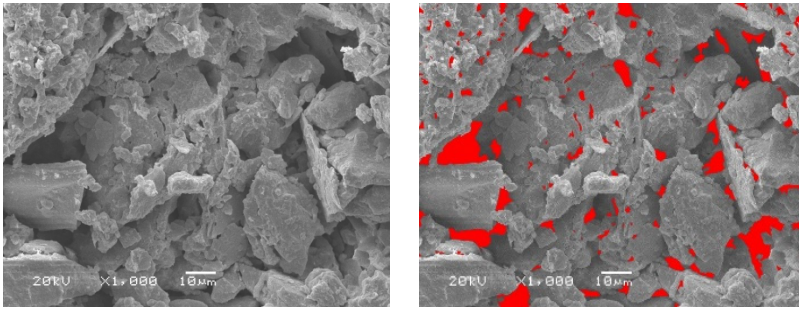
Figure 8 to 10 shows the microstructure and morphology of loess at different depths. It can be seen that as the depth increases, the compactness of loess increases, and the internal pores also decrease. When the depth reaches 20m, the pores have become very small.



(a) SEM original image

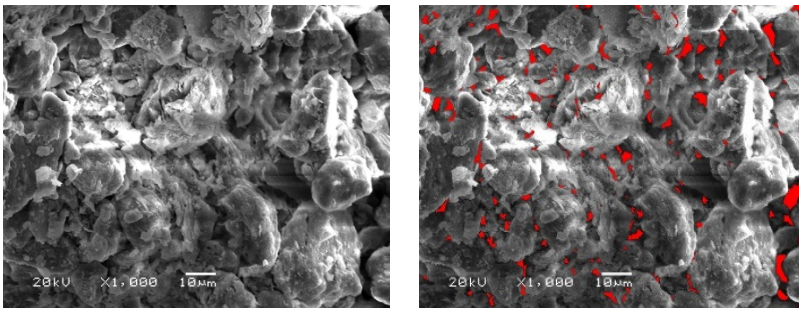
(b) After software processing

**Fig. 8.** SEM image at a depth of 5m



(a) SEM original image

(b) After software processing

**Fig. 9.** SEM image at a depth of 10m

(a) SEM original image

(b) After software processing

**Fig. 10.** SEM image at a depth of 20m

## 6 Conclusions

(1) The spherical model and exponential model are suitable for compressive modulus and natural density, the spherical model and Gaussian model are suitable for soil mass mechanical parameters, the spherical model is suitable for shear wave velocity, and the spherical model is the optimal model.

(2) The relationship between the fluctuation range of each parameter is as follows: natural density > internal friction angle > cohesion > compressive modulus.

(3) The spatial coefficient of variation of the compressive modulus is the largest, because the graded loading has an inevitable damage to the natural results of the soil during the consolidation experiment of the compressive modulus, so the variability itself becomes larger.

(4) According to the established model, the spatial variability of the soil can not be ignored in geotechnical engineering, and the spatial variation performance of soil parameters is better studied for the uncertainty of soil parameters.

## References

1. Sung E. C. "Probabilistic assessment of slope stability that considers the spatial variability of soil properties," *Journal of Geotechnical and Geoenvironmental Engineering*, 2010, 136(7) : 975-984.
2. Zhu H., Zhang L. M., Zhang L. L., et al. "Two-dimensional probabilistic infiltration analysis with a spatially varying permeability function," *Computers and Geotechnics*, 2013, 48: 249-259.
3. Wang Y., Cao Z. "Expanded reliability-based design of piles in spatially variable soil using efficient Monte Carlo simulations," *Soils and Foundations*, 2013, 53(6) : 820-834.
4. Li X. Y., Zhang L. M., Gao L., et al. "Simplified slope reliability analysis considering spatial soil variability," *Engineering Geology*, 2017, 216: 90-97.
5. Tang M. H., Lu S., "Research on the spatial distribution of slip zone of Huangtupo landslide in Three Gorges Reservoir area," *Journal of Engineering Geology*. 2018, 26(1): 129-136.
6. Yang J., Li B., Bao A. Q., et al. "Analysis of vertical bearing capacity of single pile foundations considering spatial variability of soil parameters," *Journal of Hydraulic Engineering*, 2019(05):85-90.
7. Su R., Zhang H. R., Zhang. W., et al. "Immersion tests on self-weight collapsible loess site with large depth of Lanzhou metro line," *China Civil Engineering Journal*, 2020, 53(S1) :186-193.
8. Ching J, Phoon K K. "Constructing a site-specific multivariate probability distribution using sparse, incomplete, and spatially variable (MUSIC-X) data," *Journal of Engineering Mechanics*, 2020, 146(7).
9. Zhang D. M., Dai T. F., W H., et al. " Analysis of shallow foundation bearing capacity considering geological variation". *Journal of Underground Space and Engineering*, 2020,16 (05): 1412-1419
10. Wang S. G., Xia P., Dong X. Y., et al. "Finite element analysis of the upper limit of the ultimate bearing capacity of the foundation considering spatial variability," *Journal of China & Foreign Highway*, 2021,41(04):27-31.
11. Xiao Z. Y. "Reliability analysis of foundation engineering considering soil's spatial variability," *HeFei University Of Technology*, 2022.
12. Liao Y. H. "Research on settlement and deformation of loess embankment based on spatial variability of soil parameters," *Lanzhou Jiaotong University*, 2022.
13. Chen X. Q. "Evaluation of thick loess collapse based on spatial variability of soil parameters," *Lanzhou Jiaotong University*, 2022.
14. Zhao C. "Research on the Coupling Probability Modeling Method of Stratigraphic Types and Spatial Distribution of Geotechnical Parameters Based on Random Field Theory," *China University of Geosciences*, 2022
15. Lei L., Zhen W. Q., Wu B. et al. " Study on Deformation of Subway Foundation Pit Based on Parameter Spatial Variability Random Field," *Journal of Hydroelectric Engineering*, 2023, 49(08): 42-48+113.
16. Zhu L., Gao X. Y., Wan Y. K. "Influence of Slope Height and Slope Ratio on Reliability of Channel Slopes," *Journal of Irrigation and Drainage*, 2023, 42(12): 125-131.
17. Liu J. L., Liu L., Ma X. Y. et al. " Study on spatial variability of soil salinity in different scales and soil layers. " *Chinese Journal of Applied Basic and Engineering Sciences*, 2018, 26 (02): 305-312

**Open Access** This chapter is licensed under the terms of the Creative Commons Attribution-NonCommercial 4.0 International License (<http://creativecommons.org/licenses/by-nc/4.0/>), which permits any noncommercial use, sharing, adaptation, distribution and reproduction in any medium or format, as long as you give appropriate credit to the original author(s) and the source, provide a link to the Creative Commons license and indicate if changes were made.

The images or other third party material in this chapter are included in the chapter's Creative Commons license, unless indicated otherwise in a credit line to the material. If material is not included in the chapter's Creative Commons license and your intended use is not permitted by statutory regulation or exceeds the permitted use, you will need to obtain permission directly from the copyright holder.

